IARJSET

ISSN (Online) 2393-8021
ISSN (Print) 2394-1588

International Advanced Research Journal in Science, Engineering and Technology

Vol. 8, Issue 3, March 2021

DOI: 10.17148/IARJSET.2021.8328

FABRICATION AND ANALYSIS OF SS316-CuAl BIMETALLIC WALL MADE BY METAL INERT GAS (MIG) BASED WIRE ARC ADDITVE MANUFACTURING

Karthik BS[1], Hariharan P[2], Karthikeyan M[3]

Department of Mechanical Engineering, Coimbatore Institute of Technology, Coimbatore-14[1,2,3]

Abstract: Wire arc additive manufacturing is one of the emerging and rapidly growing technology which is gradually employed in manufacturing real time products without much of material wastage especially where expensive materials are utilised like aerospace industry. Since the metal is deposited by means of welding layer by layer heating and cooling of layers occur repeatedly. This paper focuses on investigation suitability of WAAM process in producing bimetals consisting of one ferrous (SS 316L) and one non-ferrous metal (CuAl-A2). Initially a SS wall is made by layer-by-layer deposition. It is the followed depositing aluminium bronze on the lateral side of the wall by tilting the welding torch. The developed bimetallic wall is then detached from the substrate is subjected to testing and the results are discussed.

1. INTRODUCTION

Bimetals are components which are obtained by joining of two metals or alloys of different properties. Unlike alloys bimetals consists of a metallurgical bond at the interface of two metals/alloys rather than complete mixing of metals in alloys. Bimetals are an efficient method achieve the desired properties since the two metals would complement each other in terms of mechanical, physical, chemical properties and also economically. They are utilised in the form of wires, sheets, strips, pipes, rods etc. depending upon the requirement.

Wire arc additive manufacturing is an emerging technique in the fabrication of 3D metallic structures by using electric arc as heat source and wire as feedstock. The heat source may be either TIG, MIG or PAW. The complexity of the parts manufactured by this technique ranges from low to medium and the size of the parts ranges from medium to high. It is not a suitable technique for produced highly complex parts and the part size is determined by manipulator (motion control system) capacity. The materials which have been proved to be successful through WAAM are Aluminium, Steel, titanium and brass.

This experiment focuses on integration of MIG based Wire Arc Additive Manufacturing in fabricating a Bimetallic wall of a Ferrous (SS316L) and a Non-ferrous material (CuAl) and the specimen is investigated based on the certain mechanical and NDT tests to determine the feasibility of the process in producing bimetals of ferrous and nonferrous materials. The major influencing factors in MIG based WAAM are Welding Current, Welding Voltage, Welding speed, Feed Rate, Starting Current and Time, Ending current and time, Gas flow Rate and Waiting Time between each layer to be welded. The parameters for both the materials were obtained by trial-and-error method of varying voltage. A Fronius welding source was used where the welding current, feed rate varies according to the set voltage.

Table 1.1 Composition of SS316L

Elements	C	Cr	Ni	Mo	Mn	Si	P	S	Cu	Fe	Co	Ti
Composition (in wt.%)	0.042	17.04	10.38	2.21	2.21	0.374	0.018	0.015	0.0042	68.2	0.099	0.0005
Elements	Nb	V	W	Sb	Pb	B	As	Sn	Bi	Ta	Se	N
Composition (in wt.%)	0.004	0.001	0.007	0.002	0.002	0.0002	0.0015	0.0005	0.001	0.01	0.0025	0.002

Table 1.2 Composition of CuAl

Elements	Al	Fe	As	Si	Pb	Cu	Zn	P	Sn	Mn	Ni	Cr	Mg
Composition (in wt.%)	10	1.03	0.058	0.86	0.004	88.5	0.005	0.018	0.007	0.235	0.025	0.0003	0.0007

IARJSET

ISSN (Online) 2393-8021
ISSN (Print) 2394-1588

International Advanced Research Journal in Science, Engineering and Technology

Vol. 8, Issue 3, March 2021

DOI: 10.17148/IARJSET.2021.8328

2. EXPERIMENTAL SETUP AND PROCEDURE

The experimental setup consists of a Six axis ABB Robot (IRB 1520ID) with wire feeder and IRC5 controller, a Fronius TPS 400i Welding unit, Shielding Gas cylinder. The Fronius welding unit and ABB robot are interfaced and the robot motion is controlled by RAPID PROGRAM. The suitable welding parameters are saved as a job in the welding unit and utilized in program. Two separate wire spools of SS and CuAl are used whose wire diameter is 1.2 mm.

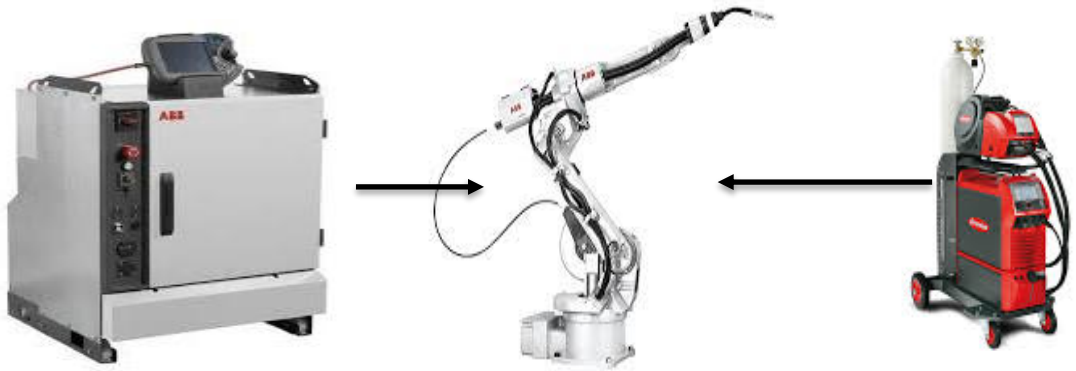

Fig 2a Integrated Welding Environment

Table 2.1 Welding parameters of SS316L and CuAl

WELDING PARAMETERS	SS316L	CuAl
Welding current	190A	340A
Welding voltage	18.3V	28.9V
Wire feed rate	6.7m/min	11.8m/min
Welding speed	4mm/s	4mm/s
Welding width and length	6mm	3mm,60mm
Starting current and time	120%, 0.3s	120%,0.3s
End current and time	100, 0.2s	100%,0.2s
Mode	Low Spatter Control	Pulse Multi Control
Weave width	6mm	3mm

Initially a 200 x 150 Mild Steel plate of 20mm thickness is chosen as substrate and is surfaced prepared for depositing the material. 20mm thickness is preferred to avoid any distortion of the plate due to high temperature generated during repeated welding cycles. The SS316L wire spool is mounted on the wire feeder and the welding parameters are set on the welding unit. SS 316 is welded using the LOW SPATTER CONTROL mode to reduce the spatter produced. The RAPID program is run and the SS WALL is deposited. A total of 9 layers are deposited whose dimensions was 60 x 11 x 29mm(l*b*h) with a waiting time of 40 seconds given in between depositing each layer to avoid distortion. Following the deposition of the SS wall the Aluminium Bronze wire spool is mounted on the wire feeder. PULSE MULTI CONTROL (PMC) is used for Aluminium bronze supply current in the form of pulses to reduce continuous power supply which provides excessive heat input to Aluminium Bronze. Since Aluminium bronze has higher thermal conductivity, heat input given should as low as possible to achieve beads of right shape or else the bead shape gets distorted. This time the end effector is tilted at an angle of 30 degree and a similar wall of 9 layers is deposited Adjacent to the SS wall with the same waiting time of 40 seconds. The bimetallic wall is then machined along the surfaces using face milling until smooth surfaces are obtained. The machined bimetallic wall is then removed from the substrate using Abrasive Waterjet Machining process. The detached specimen is then subjected to testing.

IARJSET

ISSN (Online) 2393-8021
ISSN (Print) 2394-1588

International Advanced Research Journal in Science, Engineering and Technology

Vol. 8, Issue 3, March 2021

DOI: 10.17148/IARJSET.2021.8328

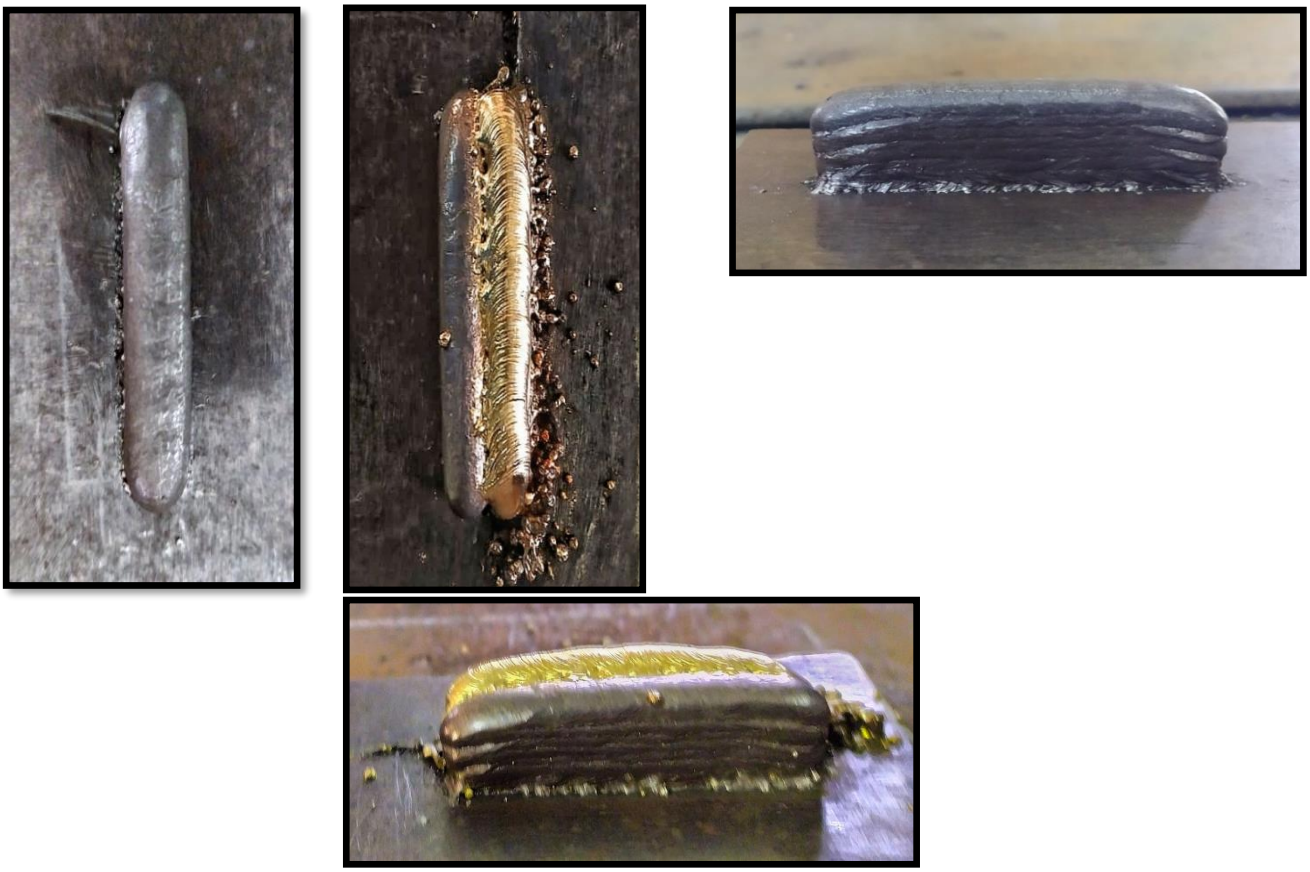

Fig 2(a)SS wall fabrication, 2(b)CuAl deposition along SS wall

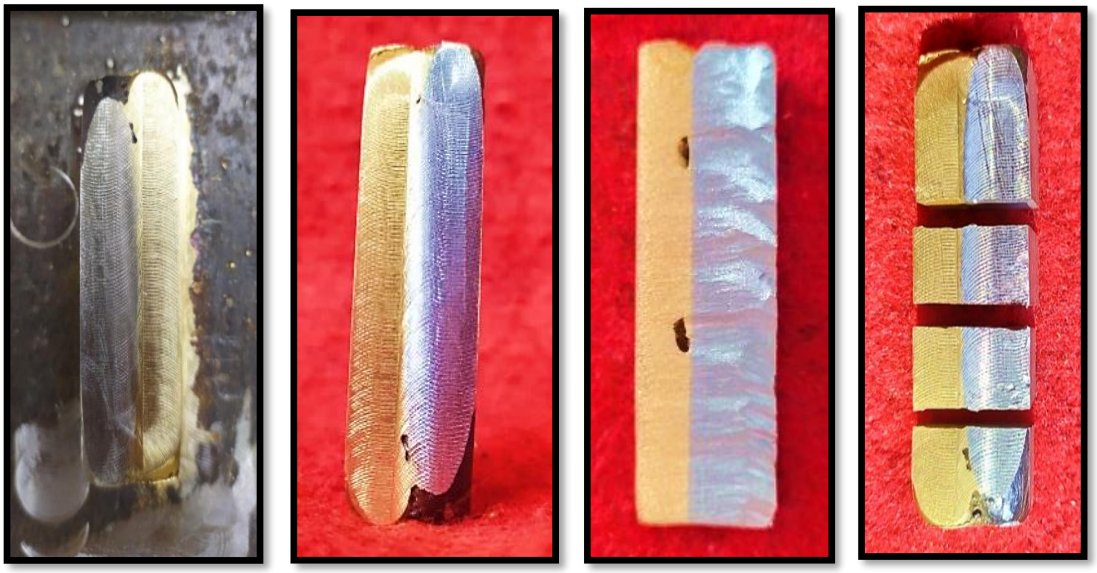

Fig 2(c) Machined bimetallic wall 2(d)Detached bimetallic wall from substrate
2(e)Bottom face of detached bimetallic wall 2(f)Sliced bimetallic wall

IARJSET

ISSN (Online) 2393-8021
ISSN (Print) 2394-1588

International Advanced Research Journal in Science, Engineering and Technology

Vol. 8, Issue 3, March 2021

DOI: 10.17148/IARJSET.2021.8328

Table 2.2 Parameters and dimensions of SS316L-CuAl bimetallic wall

S. No	Parameters	Materials	
		SS316L	CuAl
1	Density of the material(kg/cm^3)	7.990	7.529
2	Diameter of the wire used(mm)	1.2	1.2
3	Area of cross section of the wire(m^2)	1.13×10^{-6}	1.13×10^{-6}
4	Wire Feed rate(m/min)	6.7	11.8
5	Ideal Deposition Rate (kg/hr)	3.63	6.02
6	Actual Deposition Rate (kg/hr)	1	1.68
7	Dimensions before machining (l x b x h) mm	60 x 11 x 29	60 x 7 x 28
8	Weight of the wall before machining (grams)	90	70
9	Amount of raw material used in fabricating the bimetallic wall (grams)	362	
10	Final weight of the sample bimetallic wall before machining (grams)	160	
11	Final weight of the sample bimetallic wall after machining (grams)	134	

Ideal Deposition rate- Deposition rate when the material is continuously deposited without waiting time between each layer

Actual deposition rate-Deposition rate considering the waiting time given in between depositing successive layers

The reason for actual deposition rate being lower than the Ideal deposition rate is because of the longer waiting time in between the layers. The amount of material deposited and time taken for depositing each layer is also lower when compared with the waiting time which accounts for the lower deposition rate. In case of depositing a fairly medium to large sized component the waiting time will be lesser than the deposition time taken for each pass. Hence the deposition rate can be increased with real-time components. The buy to fly ratio was also found to be **2.7:1** which is very less when compared with conventional machining processes like casting. It can be further improved by optimizing the parameters and reducing the material losses that happen in the process like spatter.

3.RESULTS AND DISCUSSION

3.1 RADIOGRAPHY TEST

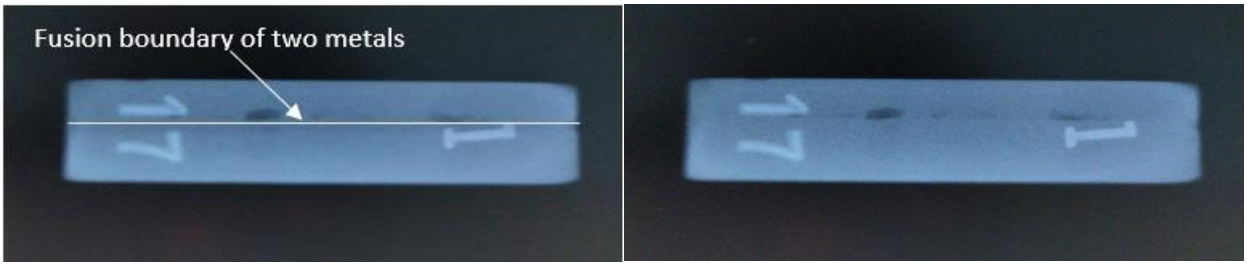

Fig 3.1 Radiograph of the bimetallic wall

The radiograph obtained shows that the metals individually are free from cracks (transverse and longitudinal) hence proving the integrity of the material and each layer has perfectly fused with the previous layer. The absence of crater is due to starting and ending current given for extended duration. Undercuts are also not spotted due to the proper dwell time given at the right, left and centre during weaving, optimal welding speed and also effective start and end current. There is no slag inclusion between the weld turns due to the exact current, welding speed and proper travel rate. The lack of penetration also shows that the parameters are suitable.

The defects that are spotted are non-uniform fusion of two metals along the fusion boundary and porosity at certain areas. The porosity is due to the weld pool turbulence and excessive gas flow rate. The non-uniform fusion is due to the inadequate data regarding the welding parameters of aluminium bronze which could be rectified by trials.

IARJSET

ISSN (Online) 2393-8021
ISSN (Print) 2394-1588

International Advanced Research Journal in Science, Engineering and Technology

Vol. 8, Issue 3, March 2021

DOI: 10.17148/IARJSET.2021.8328

3.2MICROSTRUCTURE

3.2.1 SS316L

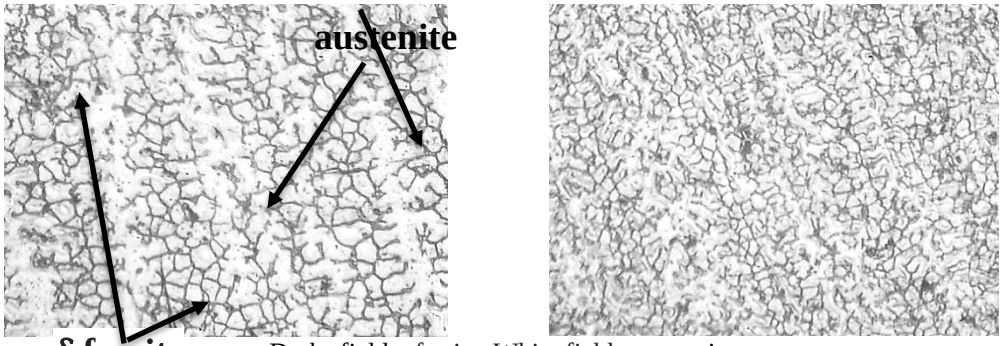

Darks fields- ferrite, White fields- austenite

Fig 7.3 Micrograph of SS316L

The obained microgarph of SS3316L exhibited Austenite and delta ferrrite microstructure. The austenite has a FCC crystal structure and it an allotrope of iron and it is created by heating ferrite to 912 degree celsius during which it takes a transition from BCC to FCC structure which can dissolve more c arbon. δ-ferrite is a high temperaturre form of iron which has BCC crystal structure is formed on cooling low carbon concentrations in iron carbon alloys from liquid state before transforming austenite. The delta ferrite can be retained at room temperature in high alloyed steels like SS316L The presence of austenite improves corrosion resisitence , strength and ductility. Delta ferrite increases the yield strength, ultimate tensile strength, increases the resistance to stress corrosion and its resultant cracking.

3.2.2 CuAl

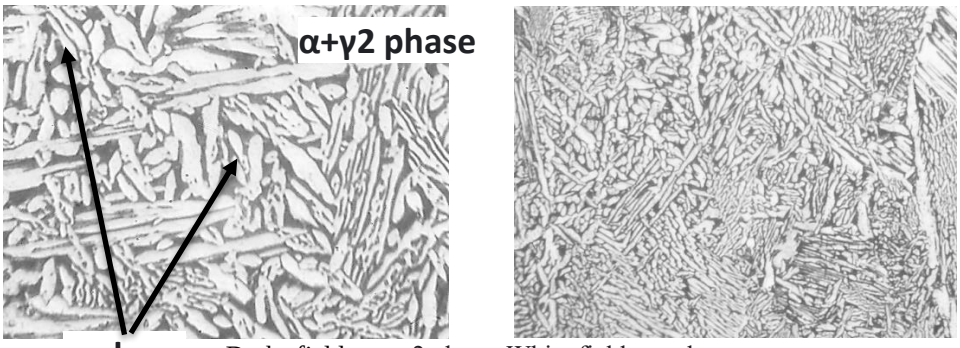

Darks fields- α+γ2 phase, White fields- α phase

Fig 7.4 Micrograph of CuAl

The micrograph of CuAl exhibited two phases namely α phase and the eutectoid(α+γ2 phase) when taken u nder magnification less than 500x. The aluminium occurs in the form solid solution in α phase and the eutectoid(α+γ2 phase). There is another phase called k-phase which is visible under magnification greater than 500x. The k-phase has BCC crystal structure and comprises copper, aluminium, iron and nickel. The best mechanical properties of aluminium bronze can be achieved when iron to nickel ratio in k- phase is greater than 1.

3.2.3 Interface

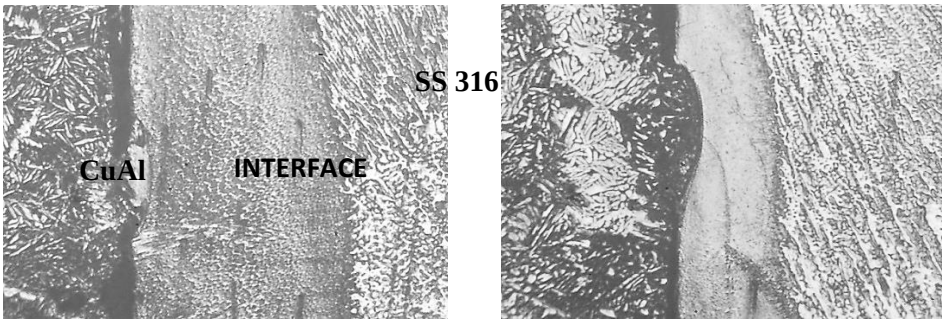

Fig 3.2.3 Micrograph of Interface of two metals

IARJSET

ISSN (Online) 2393-8021
ISSN (Print) 2394-1588

International Advanced Research Journal in Science, Engineering and Technology

Vol. 8, Issue 3, March 2021

DOI: 10.17148/IARJSET.2021.8328

The interface between the two materials was found to have different structure from that of the parent metals. The different microstructure is attributed to the compounds formed as a result of depositing the material side by side.

3.3 HARDNESS TEST

The hardness of the two materials were tested using Brinell Hardness hardness tester employing a ball indenter of 5 mm, load of 750kg and indentation time to be 15seconds as per ASTM A370:2020 standard. The average hardness of SS316L wall and CuAl wall deposited was found to be 148HBW and 138HBW respectively. When compared with hardness of casted SS(217 HBW max) and casted CuAl(195 HBW) the hardness of the WAAM produced component has exhibited lesser hardness. This is due to the nature of fabrication process being similar to annealing process which increases the ductility thereby decreasing the hardness of the material. The metal is heated during the deposition process and after a short cooling span of 40 seconds, the metal is overlayed further on the deposited layer which further increases the the temperature of the process where the temperature of the below deposited layers attain temperatures greater than the metal's recrytalization temperature but without surpassing the melting temperature. This process is repeated till the last layer is built up. Further to this the specimen is air cooled to room temperature gradually. Due to this the hardness of the entire component has decreased comparatively and can be utilized in application requiring high fracture toughness,good ductility and reduced hardness thereby improving the machinability.

3.4 SEM AND EDS

The SEM image gives a clear view of the k phase present in Aluminium bronze which comprises of elements such as copper aluminium nickel and iron. Further to SEM images the EDS mapping of the sample provided an insight of the major elements present in the sample.The EDS mapping of the sample shhows that the major portion of the bimetal included Aluminium,Chromium,Manganese, Iron,Nickel and Copper. These elements comprised of the around 95.5 total sample by weight and rest accounts for the minor elements . The absence of any oxides and other impurities indicate that the sample has escaped any sort of inclusions or impurities during the welding process therby it correponds to the fact that the shielding provided by Argon gas has been optimal to prevent any kind of oxide formation or contamination.

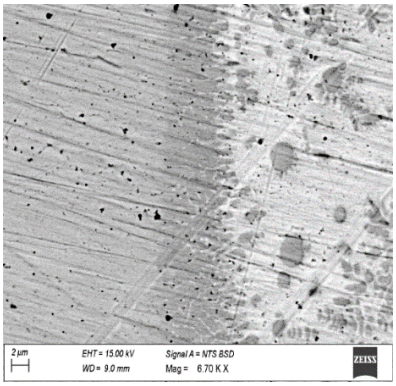

(a) SEM image of SS-CuAl sample

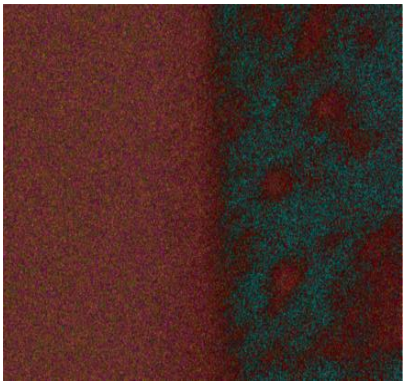

(b) EDS mapping of SS-CuAl sample

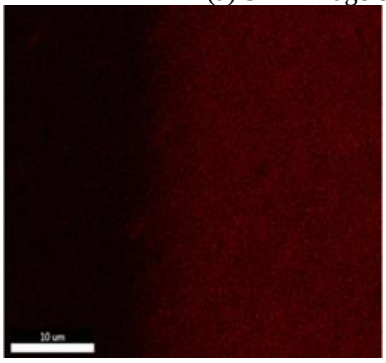

(c) Al

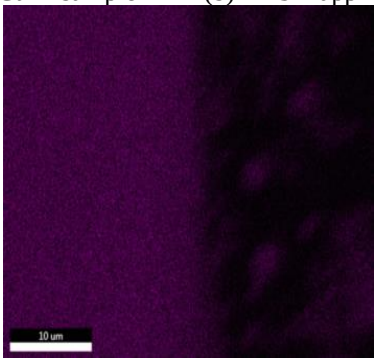

(d) Cr

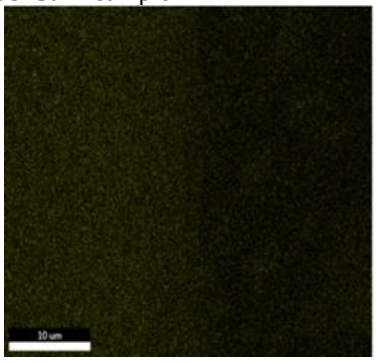

(e) Mn

IARJSET

ISSN (Online) 2393-8021
ISSN (Print) 2394-1588

International Advanced Research Journal in Science, Engineering and Technology

Vol. 8, Issue 3, March 2021

DOI: 10.17148/IARJSET.2021.8328

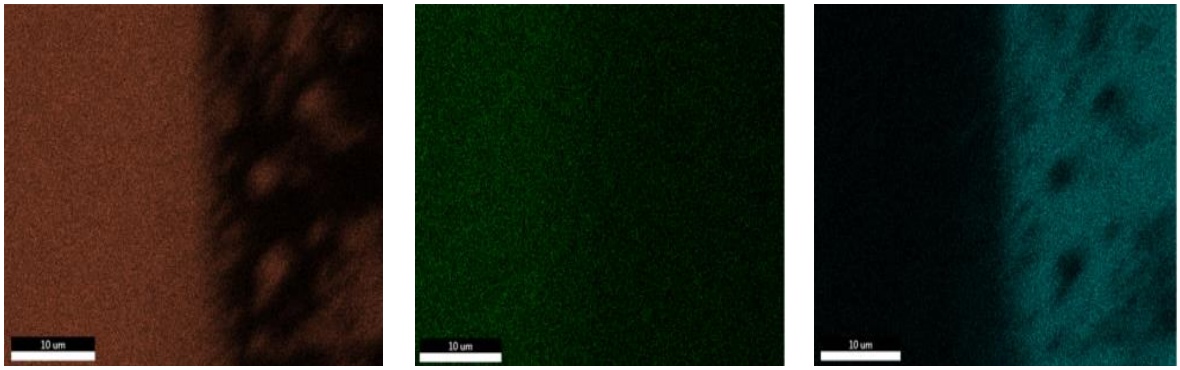

(f) Fe (g) Ni (h) Cu

Fig 3.4 (a)SEM image of bimetallic sample (b)EDS mapping of bimetallic sample
(c) to (h) - EDS mapping of Aluminium, Chromium, Manganese, Iron, Nickel, Copper respectively

The mapping also aided in finding out the weight percentage and atomic percentage of each major element. The experimental error percentage was utilized in remving the errors and the appropriate weight and atomic percentage was found for each element. The total weight of the majr elements corresponded to 95.7% by weight and 95.62% by atomic mass.

ssTable 3.4 Elements and its corresponding weight and atomic percentage

Element	Weight %	Atomic %	Error %	Corrected weight%	Corrected atomic%
Al K	3.4	7.08	8.41	3.11	6.48
Cr K	10.02	10.84	4.06	9.61	10.39
Mn K	1.41	1.44	13.71	1.21	1.24
Fe K	39.19	39.48	3.33	37.88	38.16
Ni K	6.02	5.77	7.4	5.57	5.34
Cu K	39.96	35.38	4.21	38.27	33.89

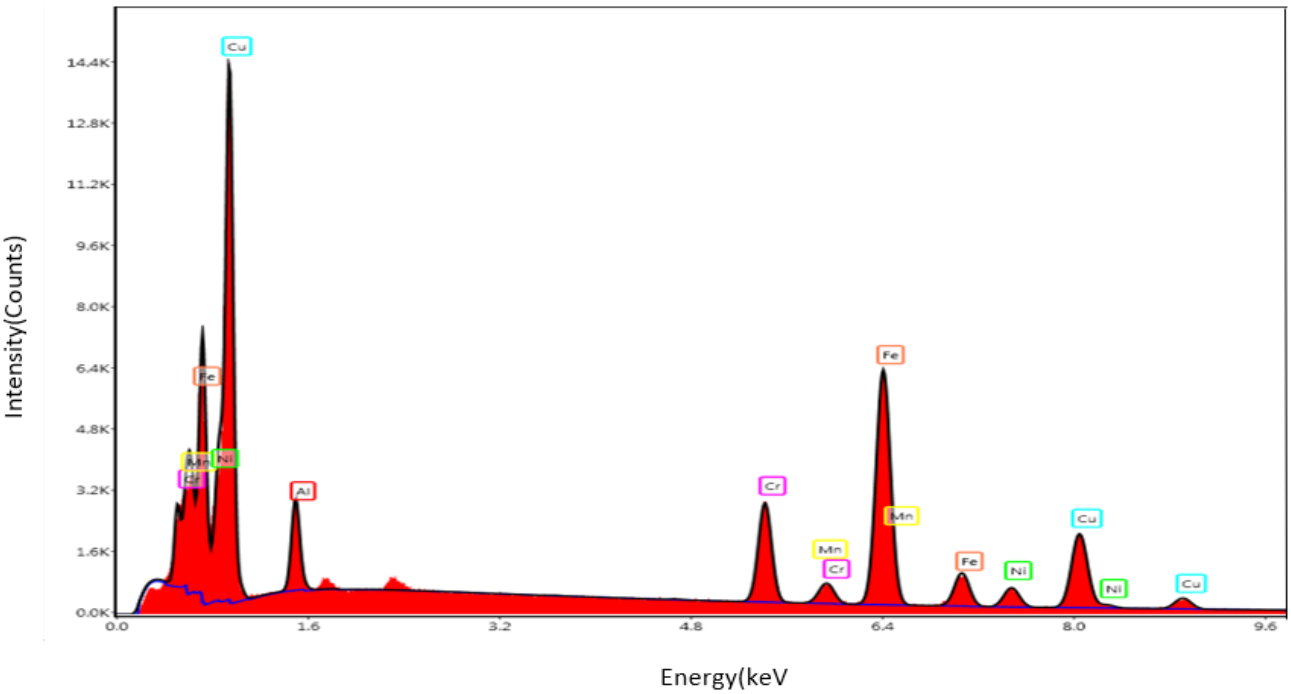

Fig 3.4 (i) EDS graph

3.5 X-RAY DIFFRACTION

The X-ray diffraction image of the sample depicts and affirms the formation of different compounds in the sample indicating that the bond formed is metallurgical bond and the two metals has fused together. The compounds that are formed are Aluminium Chromium Copper Iron ($Al_{6.5}Cr_{0.5}Cu_2Fe$), Aluminium Copper Nickel ($Al_{0.28}Cu_{0.69}Ni_{0.02}$),

IARJSET

ISSN (Online) 2393-8021
ISSN (Print) 2394-1588

International Advanced Research Journal in Science, Engineering and Technology

Vol. 8, Issue 3, March 2021

DOI: 10.17148/IARJSET.2021.8328

Aluminium Chromium Iron ($Al_{95}CrFe_4$), Iron Nickel ($Fe_{0.916}Ni_{0.084}$), Aluminium Nickel ($AlNi_3$). The crystal system, **2θ (**angle between incident and reflected x ray) at which maximum intensity and the volume of the cell of each compound formed in its crystalline structure is listed below

Table 3.5 Compounds formed in the bimetallic sample

Compounds formed	Crystal system	2θ at 100% Intensity	Volume of the cell in pm^3
Al Chromium Copper Iron	Orthorhombic	43.992	9424.19
Aluminium Copper Nickel	Cubic	42.195	51.06
Aluminium Chromium Iron	Unknown	44.142, 41.786	-
Iron Nickel	Hexagonal	50.420	18.59
Aluminium Nickel	Cubic	42.569	49.65

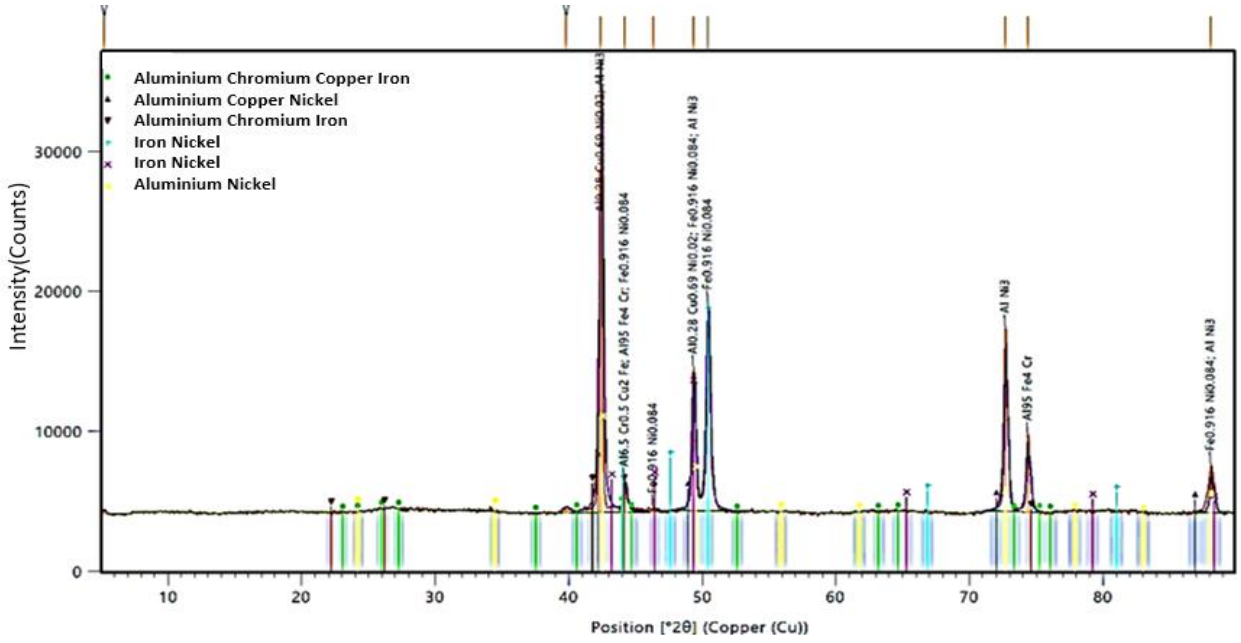

Fig 3.5 (a) Peaks obtained during X-Ray difffraction of the sample

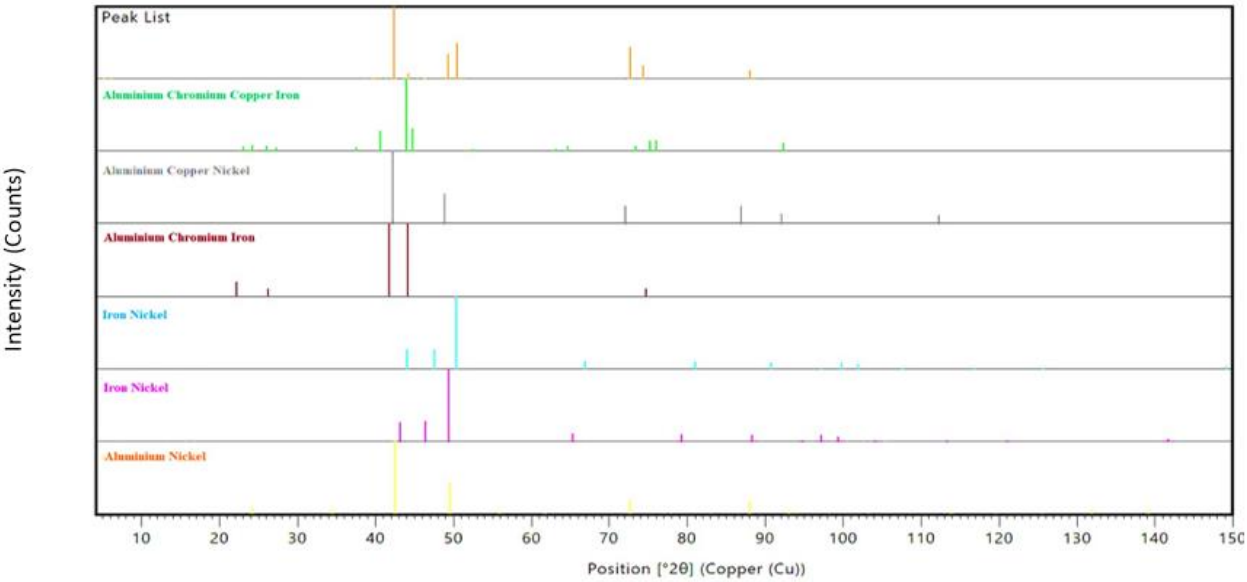

Fig 3.5 (b) Peaks of individual compounds formed

IARJSET

ISSN (Online) 2393-8021
ISSN (Print) 2394-1588

International Advanced Research Journal in Science, Engineering and Technology

Vol. 8, Issue 3, March 2021

DOI: 10.17148/IARJSET.2021.8328

The individual peaks represent that the X-rays projected exhibited maximum intensity after scattering from individuals compunds at various incident angles (θ). By using this angle and the wavelength of the incident X-ray in Braggs Law the distance between the crystal planes of the particular compound can be found which helps in determining the volume of the cell.

CONCLUSION

A bimetallic wall of SS316L and CuAl was fabricated using MIG based Wire Arc Additive Manufacturing and the following results were obtained as a result of the experimental tests and analysis.

1. A strong metallurgical bond was created between the two metals as a result of which several intermetallic compounds were forrmed inspite of the non uniform bond along the fusion bounndary at some places.
2. A appreciable buy to fly ratio of 2.7:1 was achieved which can be further improved by optimising the welding process and its paramters and determining better means to reduce the spatter.
3. The sample achieved was nearly defect free without any sort of major inclusions like oxides and slags.
4. The process exhibited samples with reduced hardness which improves the machinability and being resisitant to higher impact. Depending upon the applications the hardness can be increased by suitable heat treatment processes.
5. The further scope of the work involves builiding bimetals which can be utilized in real time applications like bearings etc.. with uniform fusion along the boundaries

REFERENCES

[1]. Giuseppe Venturinia, Filippo Montevecchia, Antonio Scippaa, Gianni Campatellia, Optimization Of WAAM Deposition Patterns For T-crossing Features,5th CIRP Global Web Conference Research and Innovation for Future Production, ScienceDirect, 95-100,2016

[2]. Bintao Wu, Donghong Ding, Zengxi Pan, Dominic Cuiuri, Huijun Li, Jian Han, Fei, Effects Of Heat Accumulation On The Arc Characteristics And Metal Transfer Behavior In Wire Arc Additive Manufacturing Of Ti6al4v, Journal of Materials Processing, ScienceDirect, 305-312, 2017

[3]. Zeqi Hua, Xunpeng Qina, Tan Shaoa, Welding Thermal Simulation and Metallurgical Characteristics Analysis in WAAM for 5CrNiMo Hot Forging Die Remanufacturing, International Conference on Technology of Plasticity, ScienceDirect, 2203-2208, 2017

[4]. José Luis Prado-Cerqueira, Ana María Camacho 1, José Luis Diéguez , Álvaro Rodríguez-Prieto 1,3, Ana María Aragón, Cinta Lorenzo-Martín and Ángel Yanguas-Gil, Analysis of Favorable Process Conditions for the Manufacturing of Thin-Wall Pieces of Mild Steel Obtained by Wire and Arc Additive, Materials, 2018

[5]. Manufacturing (WAAM)J. Nazari, M. Yousefi', M.S. Amiri Kerahroodi', N.S. Bahrololoumi Mofrad, S.H. Alavi Abhari, Production of Copper-Aluminum Bimetal by Using Centrifugal Casting and Evaluation of Metal Interface, International Journal of Material Lifetime, Vol 1,20-28, 2015

[6]. Dmitriy Nikolayevich Trushnikov, Elena Georgieva Koleva, Roman Pozolovich Davlyatshin, Roman Mikhailovich Gerasimovand Yuriy Vitalievich Bayandin, Mathematical modeling of the electron-beam wire deposition additive manufacturing by the smoothed particle hydrodynamics method, Mechanics of Advanced Materials and Modern processes, 2019

[7]. Shubham Dahat, Kjell Hurtig, Joel Andersson and Americo Scotti, A Methodology to Parameterize Wire + Arc Additive Manufacturing: A Case Study for Wall Quality Analysis, Journal of Manufacturing and Materials Processing, 2020, 10.3390/JMMP4010014

[8]. T. Ramkumar, M. Selvakumar, P. Narayanasamy, A. Ayisha Begam, P. Madhavan, Studies on the structural property, mechanical relationships and corrosion behaviour of Inconel 718 and SS 316L dissimilar joints by TIG welding without using activated flux, Journal of Manufacturing Processes, 2017

[9]. J. Łabanowski, T. Olkowski, EFFECT OF CHEMICAL COMPOSITION AND MICROSTRUCTURE ON MECHANICAL PROPERTIES OF BA1055 BRONZE SAND CASTINGS, ADVANCES IN MATERIALS SCIENCE, Vol. 9, No. 1(19), March 2009